JOURNAL OF CATALYSIS 134, 409–421 (1992)

Thermal Desorption and Infrared Studies of Amines Adsorbed on SiO_2, Al_2O_3, Fe_2O_3, MgO, and CaO

IV. Allylamine and Benzylamine

ROLF SOKOLL AND HARTMUT HOBERT

Institut für Physikalische Chemie, Chemische Fakultät, Friedrich-Schiller-Universität Jena, Lessingstrasse 10, O-6900 Jena, Germany

Received February 13, 1990; revised October 11, 1991

Adsorption of allylamine and benzylamine on SiO_2, Al_2O_3, Fe_2O_3, MgO, and CaO at the solid/vapor interface has been studied by infrared spectroscopy and temperature-programmed desorption. At beam temperature similar surface complexes are formed as in previous work with other amines. Compared to saturated amines, more reactions take place with increasing temperature during the TPD runs; these include dehydrogenation to the corresponding nitriles and CN bond breakage. Besides gaseous NH_3, in the latter reaction allyl and benzyl species, respectively, that undergo several further chemical transformations on the oxide surfaces are formed. Allylamine/MgO and allylamine/CaO are the only systems (of all investigated amine/oxide systems) in which surface reactions begin already at room temperature.

INTRODUCTION

In Parts I–III (*1–3*) we have shown that the molecular structure of simple amines does not influence the nature of their adsorption on oxides at ambient temperature, but differences emerge when the adsorbates are heated and desorption is monitored. Distinctions then occur depending on whether the original amine was primary, secondary, or tertiary, as well as on the nature of the alkyl or aryl moiety. In the present part, the study is completed by an investigation of the adsorption and decomposition of allylamine and benzylamine, whose C–N bonds are weaker than those of the amines studied previously. Some general conclusions are then drawn.

EXPERIMENTAL

The preparation and pretreatment of the oxides, the dosing and measuring procedures, and the instrumentation were basically as described in Part I (*1*). Temperature-programmed desorption (TPD) and infrared (IR) spectroscopic measurements were made in association with mass spectrometric (MS) analysis to define more precisely the desorption phenomena occurring with each oxide after adsorption of allylamine (AA) or benzylamine (BZA), respectively.

RESULTS

As with diethylamine (*1*), the interaction of both AA and BZA on SiO_2 showed hydrogen bonding and dissociative adsorption, while on the other oxides (γ-Al_2O_3, α-Fe_2O_3, MgO, and CaO) coordinative adsorption with Lewis sites of different acidity occurred. In the following sections, therefore, we present only those results that are characteristic of AA and BZA, respectively.

Allylamine

Table 1 summarizes the wavenumber values of the most important IR bands appearing after adsorption of AA on the various oxides and subsequent evacuation at beam temperature. Substances that desorb during the TPD runs are listed in Table 2.

The most intense TPD maximum of the system AA/Al_2O_3 (Fig. 1, peak AI) com-

0021-9517/92 $3.00

TABLE 1

Wavenumbers (cm^{-1}) of Infrared Bands of Allylamine after Adsorption at Beam Temperature, of Gaseous Allylamine, and of Adsorbed Reaction Products Formed at Elevated Temperatures

Wavenumber (cm^{-1})					
Gaseous allylamine	SiO_2	Al_2O_3	Fe_2O_3	MgO	Assignment
—	3439	—	—	—	ν(NH)/1 sec amine
3409	3370	3324	3328	3337	$\nu_{as}(NH_2)$
3345	3302	3230	3229	3268	$\nu_s(NH_2)$
—	—	3127	3130	—	$2\delta(NH_2)$
3083	3082	3078	3078	3079	$\nu(=CH_2)$
—	—	1651	—	1656	ν(C=N)/imine
1638	1638	1637	1637	1637	ν(C=C)
—	—	1619	—	—	ν(C=C)/aromatic
—[a]	1589	1584	1584	1587	$\delta(NH_2)$
—	—	1560	1538	—	$\nu_{as}(COO^-)$
—	—	—	—	1557	ν(C⋯C⋯C)/π-allyl
—	1550	—	—	1557	$\delta(NH_2)$[b]
—	—	—	—	1517	ν(C⋯C⋯C)/π-allyl
—	—	1485	1487	—	ν(C=C)/aromatic
—	—	1457	—	—	ν(C=C)/aromatic
—	—	—	—	1455	$\delta_{as}(CH_3)$, $\delta_s(CH_2)$
—	—	—	1423	—	$\nu_s(COO^-)$
1420	1419	1417	1417	1417	$\delta(=CH_2)$
—	—	—	—	1372	$\delta_s(CH_3)$

[a] $\delta(NH_2)$ of gaseous allylamine is partly masked by the ν(C=C), and therefore an exact wavenumber cannot be given.

[b] Absorptions of surface NH_2 groups.

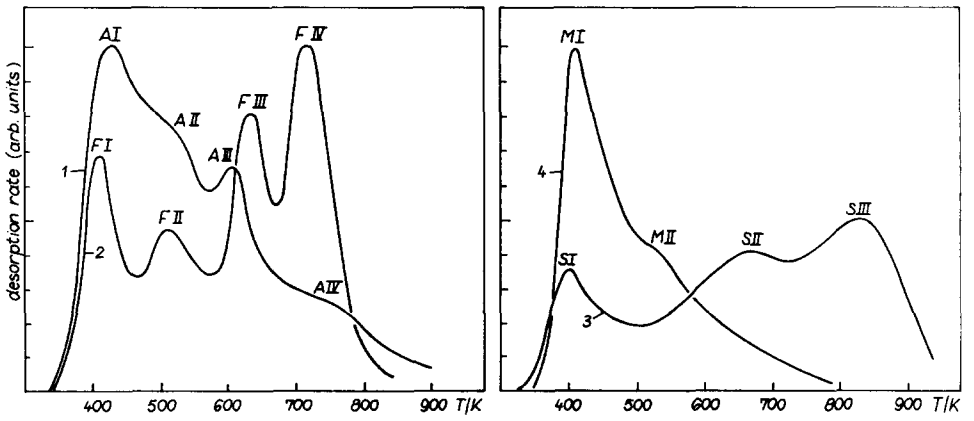

FIG. 1. Thermal desorption curves of allylamine adsorbed on oxides at room temperature: (1) Al_2O_3; (2) Fe_2O_3; (3) SiO_2; (4) MgO.

TABLE 2

Adsorption of Allylamine on Oxides: Distribution of the Desorption Products

Desorption product	Temperature of the desorption maximum (K)			
	SiO_2	Al_2O_3	Fe_2O_3	MgO
Allylamine	403 673	433	413	413
Ammonia	(843)	533	443	393
Propylene	843	603 (533)	(443)	523
Propionitrile	793	603	513	413 523
Methylpyridine	—	753	513	—
Dimethylethylpyridine	—	—	—	413
Propylamine	—	—	—	(413)
Diallylamine	—	—	—	(413)
Carbon dioxide	—	—	633 713	—
Water	—	—	633 (713)	—
Ethylene	843	—	—	—
Hydrogen cyanide	843	—	—	—

Note. Parentheses signify product present only in small amount.

prises unchanged AA (molecules bonded to weak Lewis acid sites). In line with this, the IR spectra show decreasing intensities of all bands of adsorbed AA up to ca.473 K (Fig. 2, curves 2,3). Beginning with the latter temperature, desorption of NH_3 can be detected with a maximum at ca. 533 K (Fig. 1, peak AII). The IR spectrum recorded at 573 K (Fig. 2, curve 4) shows stronger changes than that at 473 K: there is further decrease of the AA bands and new absorptions at 1651, 1619, 1560, 1485, and 1457 cm^{-1}. Between 573 and ca. 633 K (TPD maximum AIII is located at ca. 603 K) complete degradation of adsorbed unchanged AA occurs, and the IR band at 1651 cm^{-1} also disappears. Finally, the remaining adsorptions (1619, 1560, 1485, 1457 cm^{-1}) diminish simultaneously with the desorption of an aromatic compound between 653 and 853 K (TPD maximum AIV).

With Fe_2O_3 the AA TPD is unusual in that the most intense desorption maxima are due

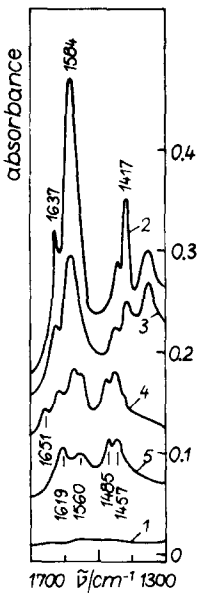

FIG. 2. Infrared spectra of Al_2O_3: (1) in vacuum, after adsorption of allylamine from the vapor phase and subsequent evacuation at (2) beam temperature, (3) 473 K, (4) 573 K, (5) 673 K.

to the oxidation products CO_2 and H_2O (Fig. 1, peaks FIII, FIV). Moreover, in contrast to the behavior of the corresponding primary amine, the FII peak comprises only a little propionitrile, but is mainly methylpyridine. NH_3 is detectable from ca. 393 K, confirming amine decomposition already below 400 K; adsorbed carboxylates are formed, as shown by Fig. 3B, curve III, where carboxylate bands at 1538 and 1423 cm^{-1} dominate the spectrum already at 443 K, the temperature of maximum NH_3 desorption.

With the alkaline earth oxides, AA, in contrast to other amines (*1–3*), shows high reactivity. Although the shape of the TPD response on MgO (Fig. 1, curve 4) is the same as that with other amines, the MI peak is no longer due only to the unchanged amine but also comprises reaction products (Table 2). Already at ambient temperature, adsorbed AA gives a slow reaction releasing NH_3, and at the same time both the MS m/z signals and the IR bands of unchanged AA diminish. In line with this, the IR spectrum after 1 min contact at beam temperature (Fig. 4, curve 2) shows not only the dominant bands (1637, 1587, and 1416 cm^{-1}; Fig. 4, curve 2) due to unchanged AA (cf. AA on Al_2O_3) but also shoulders at ca. 1656 and 1557 cm^{-1}, a small absorption at 1517 cm^{-1}, and two strong bands due to saturated alkyl groups (absent in AA itself) at 1455 and 1372 cm^{-1}. The latter increase with increasing time of contact, whereas the bands characteristic of unsaturated alkyl groups (1637 and 1416 cm^{-1}; see Table 1) diminish. After desorption up to 493 K and cooling to beam temperature the spectrum shows only small absorptions (Fig. 4, curve 3), and these also vanish on heating to 573 K.

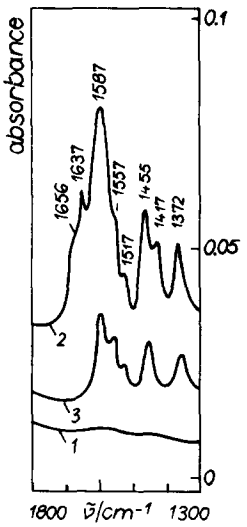

FIG. 4. Infrared spectra of MgO: (1) in vacuum, after adsorption of allylamine from the vapor phase (1-min contact between allylamine and MgO) and subsequent evacuation at (2) beam temperature, (3) 493 K.

Compared to other amine/oxide systems, AA adsorbed on SiO_2 does not show such peculiar reaction behavior as that with the other oxides. As usual (*4*), TPD maxima SI and SII (Fig. 1, curve 3) comprise AA itself (SI, hydrogen-bonded molecules; SII, recombination from OH groups and secondary amine species formed by dissociative adsorption of AA on strained siloxane bridges), and in the temperature range of SIII decomposition of the secondary amine species leads to the desorption of various products (Table 2) according to the following scheme:

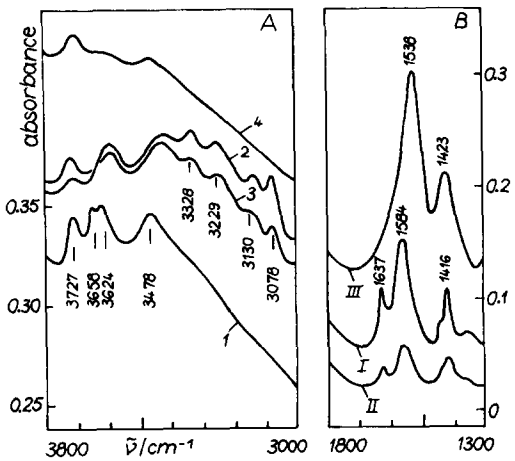

FIG. 3. (A) Infrared spectra of Fe_2O_3: (1) in vacuum, after adsorption of allylamine from the vapor phase and subsequent evacuation at (2) beam temperature, (3) 373 K, (4) 443 K. (B) Difference spectra: I = (2) − (1); II = (3) − (1); III = (4) − (1).

$$CH_2{=}CHCH_2NH{-}Si\equiv \xrightarrow{(a)} CH_3CH_2CN_{(g)}$$
$$\xrightarrow{(b)} CH_2{=}CHCH_{3(g)} + (NH_{3(g)}/{-}Si{-}NH_2) \quad (1)$$
$$\xrightarrow{(c)} CH_2{=}CH_{2(g)} + HCN_{(g)}$$

where (g) signifies gaseous species. Partial formation of surface NH_2 groups (Eq. (1b)) is indicated by the appearance of a new IR band at 1550 cm^{-1} due to a corresponding deformation vibration (*5*).

Benzylamine (BZA)

Table 3 shows that the second TPD maximum of each BZA/oxide system (with the exception of SiO_2; Fig. 5) comprises large amounts of benzonitrile formed by dehydrogenation of strongly adsorbed BZA molecules. In addition, some other phenomena obviously result from the structural peculiarities of BZA and manifest themselves by the following IR (Table 4) and MS (Table 3) data. Thus with Fe_2O_3 besides benzonitrile considerable amounts of NH_3 desorb (maximum at ca. 493 K). The IR spectra show that up to ca. 453 K (desorption of only unchanged BZA) all bands of adsorbed BZA diminish (Fig. 6, curves I,II), but already with the beginning of the NH_3 desorption strong absorptions appear at 1589, 1526, and 1402 cm^{-1} (Fig. 6, curve III/493 K). Because of the occurrence of reduction in overall spectral transmission (*1*), further reactions at higher temperatures cannot be followed up by IR spectroscopy. In contrast to aliphatic amines, desorbing CO_2 and H_2O cause a shoulder at 673 K in the TPD curve and also an intense maximum at 718 K (Fig. 5, curve 2). Furthermore, gaseous benzene causing a separate TPD maximum is detected by MS (Fig. 5, peak FIII).

Similar reaction routes occur in the system BZA/Al_2O_3. Besides dehydrogenation of strongly coordinated BZA molecules to

TABLE 3

Adsorption of Benzylamine on Oxides: Distribution of the Desorption Products

Desorption product	Temperature of the desorption maximum (K)				
	SiO_2	Al_2O_3	Fe_2O_3	MgO	CaO
Benzylamine	413 678	453	443	423	423
Ammonia	(838)	533	493	(533)	(533)
Benzonitrile	818	603	513	533	533
Benzene	(838)	603 838	643	—	—
Toluene	(838)	(603)	(513)	(533)	(533)
Hydrogen cyanide	(838)	(603)	(513)	—	—
Methane	(838)	—	—	—	—
Carbon dioxide	—	838	(643) 718	—	—
Water	—	—	718	—	—

Note. Parentheses signify product present only in small amount.

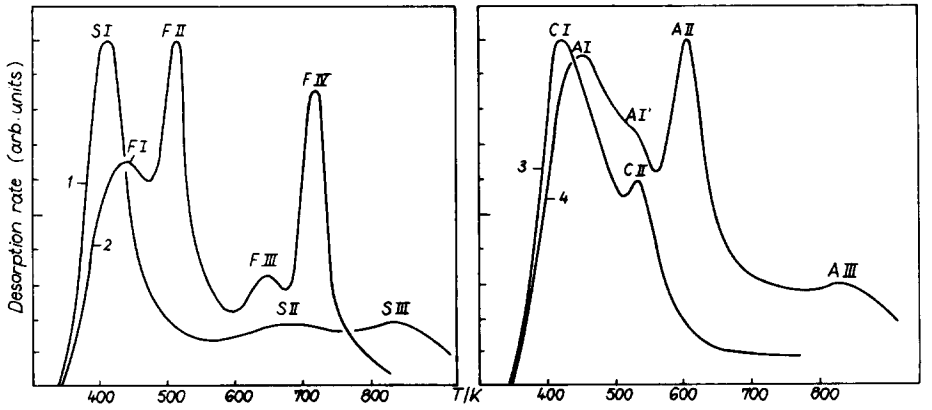

FIG. 5. Thermal desorption curves of benzylamine adsorbed on oxides at room temperature: (1) SiO_2; (2) Fe_2O_3; (3) CaO; (4) Al_2O_3.

benzonitrile (intermediate formation of adsorbed imine species is indicated by a (C=N) IR band at 1635 cm^{-1}; Fig. 7B, curve II), NH_3 desorbs with the maximum at 533 K (Fig. 5, peak AI'). Contrary to Fe_2O_3 the IR spectrum recorded at a temperature above that of the NH_3 desorption maximum only shows weak bands at 1595, 1556, and ca. 1430 cm^{-1} besides the imine absorption and $\delta(NH_2)$ at 1578 cm^{-1} of adsorbed BZA (Fig. 7B, curve 2). Moreover, at still higher temperatures a joint desorption of benzene

TABLE 4

Wavenumbers (cm^{-1}) of Infrared Bands of Benzylamine after Adsorption on Oxides at Beam Temperature and of Adsorbed Reaction Products Formed at Elevated Temperatures

Wavenumber (cm^{-1})					
SiO_2	CaO	MgO	Fe_2O_3	Al_2O_3	Assignment
3631	—	—	—	—	ν(OH)/π-interaction
3432	—	—	—	—	ν(NH)/secondary amine
3360	3338	3336	3316	3312	$\nu_{as}(NH_2)$
3297	3255	3254	3242	3239	$\nu_s(NH_2)$
3167	3138	3137	3124	3110	$2\delta(NH_2)$
3063	3064	3064	3064	3065	ν(=CH)
3027	3030	3030	3031	3031	ν(=CH)
—	—	—	—	1635	ν(C=N)/imine
—	—	—	1589	1595	ν(C=C)/benzoate; benzyl species
1587	1590	1590	1585	1582	$\delta(NH_2)$
—	—	—	—	1556	benzyl species
—	—	—	1526	1542	$\nu_{as}(COO^-)$/benzoate
—	—	—	—	1498	ν(C=C)/benzoate
1489	1490	1490	1491	1493	ν(C=C)
1448	1449	1449	1449	1451	ν(C=C)
—	—	—	1402	1432	$\nu_s(COO^-)$; CO_3^{2-}
1352	1352	1352	1353	1357	ν(C=C)

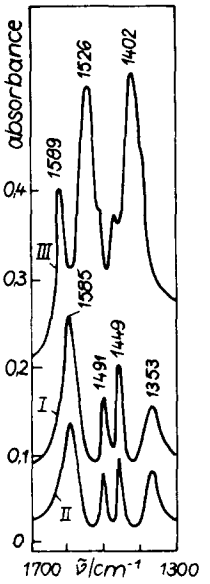

FIG. 6. Difference spectra: I = (2) − (1); II = (3) − (1); III = (4) − (1). Infrared spectra of Fe_2O_3: (1) in vacuum; after adsorption of benzylamine from the vapour phase and subsequent evacuation at (2) beam temperature, (3) 453 K, (4) 493 K.

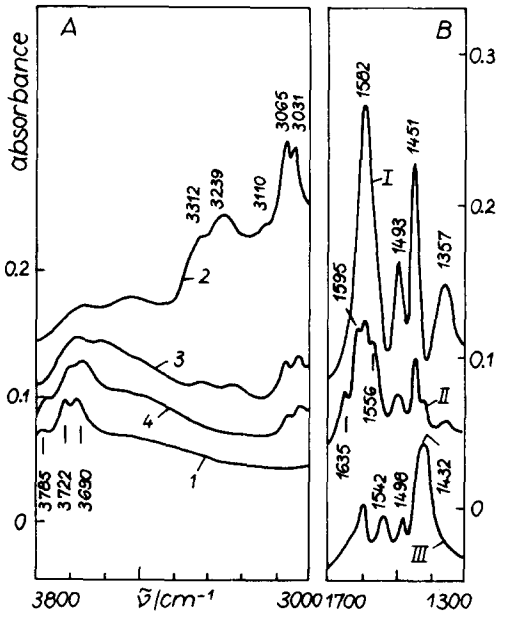

FIG. 7. (A) Infrared spectra of Al_2O_3: (1) in vacuum, after adsorption of benzylamine from the vapor phase and subsequent evacuation at (2) beam temperature, (3) 583 K, (4) 718 K. (B) Difference spectra: I = (2) − (1); II = (3) − (1); III = (4) − (1).

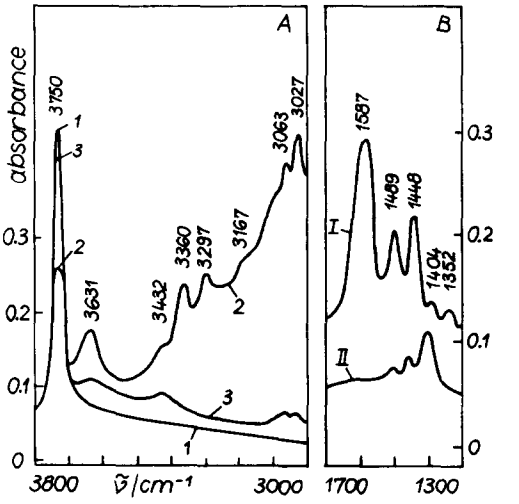

FIG. 8. (A) Infrared spectra of SiO_2: (1) in vacuum, after adsorption of benzylamine from the vapor phase and subsequent evacuation at (2) beam temperature, (3) 603 K. (B) Difference spectra: I = (2) − (1); II = (3) − (1).

and benzonitrile can be detected. After that desorption, formation of a new band at 1432 cm^{-1} and smaller absorptions at 1595, 1542, and 1498 cm^{-1} can be observed (Fig. 7, curve III). Finally, a small TPD maximum (Fig. 5, peak AIII) is caused by desorption of benzene and CO_2.

With MgO and CaO the IR spectra show a continuous decrease of all bands of adsorbed BZA with increasing temperature. Benzonitrile alone causes the second TPD maximum (Fig. 1, peak CII), whereas benzene is not in evidence as a desorption product. In conjunction with only very small amounts of desorbing NH_3 the latter show that in the case of BZA/Al_2O_3, Fe_2O_3 benzene is formed from those molecule fragments that remain on the oxide surfaces after abstraction of NH_3 from adsorbed BZA.

In the IR spectra of BZA/SiO_2 (Fig. 8) an absorption at 3631 cm^{-1} appears besides the bands of hydrogen-bonded (3360, 3297, 3167, 1587 cm^{-1}) and dissociatively adsorbed (3432, 1404, cm^{-1}) amine. This band can be attributed to surface hydroxy groups

of SiO_2 interacting with the π-system of BZA molecules (*6*).

DISCUSSION

Allylamine (AA)

The (C=C) IR band of both adsorbed and gaseous AA appears at the same wavenumber value, thus indicating no remarkable participation of this functional group in the adsorption process.

As in the case of other amines a dehydrogenation reaction of AA molecules adsorbed on strong Lewis acid sites of Al_2O_3 occurs at elevated temperatures with an intermediate formation of adsorbed imine species. This is shown both by the appearance of a weak (C=N) absorption (1651 cm^{-1}) in the IR spectrum (573 K; Fig. 2, curve 4) and by desorption of propionitrile. The latter refers to a hydrogenation of the (C=C) group. However, contrary to saturated aliphatic *n*-amines a CN bond breakage occurs as a competitive reaction, which can be detected by the already mentioned desorption of NH_3,

$$CH_2{=}CHCH_2NH_{2(a)} \xrightarrow{+H} NH_{3(g)} + CH_2{\cdots}CH{\cdots}CH^{(r/i)}_{2(a)} \quad (2)$$

where (a) signifies adsorbed, (g) signifies gaseous, and (r/i) signifies radical or ion.

The experimental data show that the formed allyl fragments (the nature of which is not clear) may react further in different ways. Thus desorption of propene indicates a possible intermediate adsorption of allyl species on Al_2O_3 forming different surface complexes (*7, 8*). It is known that especially π-allyl complexes on Al_2O_3 possess a high thermal stability (*9, 10*), and, e.g., thermal degradation of π-allyl complexes on ZnO surfaces leads to desorption of propene (*11*). On the other hand, with the desorption of NH_3 new IR bands become visible at 1619, 1485, 1457 cm^{-1} (Fig. 2, curve 4). Comparison experiments (IR spectroscopic investigation of the adsorption of 2-methylpyridine on Al_2O_3) showed that these bands are due to adsorbed methylpyridine obviously formed by reaction of allyl species with AA molecules (or imine species). The previously mentioned desorption of an aromatic compound, which is identified as methylpyridine by MS, confirms the IR result. Occurrence of such dimerization and cyclization reactions is not surprising, because conversions of C_3-hydrocarbons, especially, on solid surfaces to aromatic compounds were also described by other authors (e.g., (*12–14*)). Thus the reactions of allyl species formed by CN bond breakage can be summarized in the following scheme:

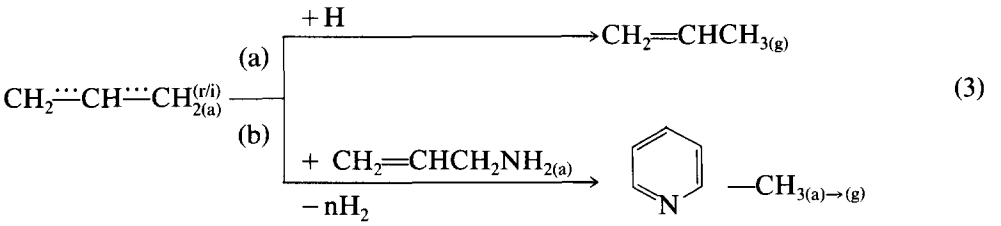

(3)

Finally, the weak IR band at 1560 cm^{-1} refers to a formation of small amounts of adsorbed propionate species (deduced from measurements with propionic acid).

The results of the system AA/Fe_2O_3 show that the same reactions occur as with Al_2O_3. However, CN bond breakage (indicated by NH_3 desorption) takes place to a remarkably greater extent, for which reason propionitrile (dehydrogenation reaction) can be de-

tected only in very small amounts. The formed allyl species further react in two ways: they are oxidized to adsorbed carboxylate species and dimerization/cyclization reactions result in the formation of methylpyridine

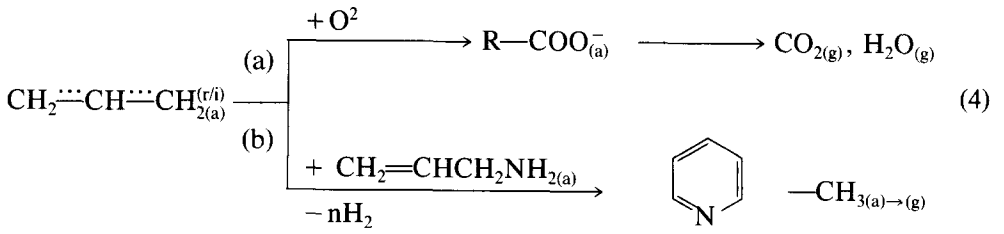

(4)

where O^{2-} signifies lattice oxygen of Fe_2O_3. That is, after the rate-determining CN bond breakage (*15*) the formed allyl species are oxidized to a great extent and an intense TPD maximum appears comprising CO_2 and H_2O (Fig. 1, peak FIII).

Finally, in contrast to all other investigated aliphatic amines, TPD maximum FIV (as well as desorption of CO_2 and H_2O) seems to be unusually intense. This can be attributed to the formation and subsequent oxidation of methylpyridine, because in the case of aromatic amines oxidation products only cause one TPD maximum at those temperatures (*3*). Discussion of the system AA/MgO can only be an attempt to interpret the very complex experimental results. Thus the nature of the identified desorption products belies various chemical transformations, which begin at room temperature and only lead to the evolution of gaseous NH_3. All other resulting products remain on the MgO surface, where their concentrations should increase with extension of the contact time between amine and MgO because of the continuous NH_3 formation. Infrared bands at 1656, 1557, 1517, 1455, and 1372 cm^{-1} (Fig. 4, curve 2) show a corresponding behavior. The absorption at 1656 cm^{-1} is probably caused by imine species, whereas that at 1557 cm^{-1} may be interpreted in two ways. On the one hand, NH_2 groups formed by dissociative adsorption of NH_3 absorb in this frequency range (*16*). On the other hand, investigations concerning the adsorption of propene on MgO showed that such a band (1555 cm^{-1}) appears with π-allyl complexes (*17*) (higher alkenes on MgO: 1555 cm^{-1} (*18*)). The latter seems more likely, because of the additional existence of an absorption at 1517 cm^{-1} (IR spectra of allyl-Mg compounds: $(C_3H_5)_2Mg$, 1540, 1510 cm^{-1}; C_3H_5MgCl, 1540, 1512 cm^{-1} (*19*). Finally, the increasing intensity of the bands at 1455, 1372 cm^{-1} illustrates the presence of processes forming saturated alkyl groups.

The observed phenomena enable us to propose the following reactions:

(a) formation of adsorbed imine species by dehydrogenation and subsequent desorption of propionitrile (TPD maximum at 413 K);

(b) hydrogenation, leading to adsorbed propylamine, which partly desorbs unchanged (maximum at 413 K) and partly reacts to desorb as propionitrile at 523 K (since only at this temperature is nitrile formed from *n*-amines);

(c) formation of gaseous NH_3 and adsorbed allyl species by CN bond breakage;

(d) formation of 2,4-dimethyl-6-ethylpyridine (main desorption product) from precursors (diallylamine, allyl species) immediately at the moment of desorption, as shown by the fact that no IR bands of adsorbed alkylpyridine can be detected.

Literature data confirm the possible occurrence of these reactions. Thus MgO acti-

vated at 1073 K shows high activity already at 300 K for selective catalytic hydrogenation of alkenes by H_2 (*20, 21*). Furthermore, because of the basic character of MgO, many adsorbed molecules interact heterolytically with the surface metal cations and oxygen anions; e.g., alkenes are dissociatively adsorbed at room temperature (*22*). Finally, in addition to knowledge of dimerization of allyl species on MgO (*22*), polymerization of styrene (*23*) and acetylene (*24*) and formation of methyl- and dimethylpyridine from allylamine (*25*) are known.

Benzylamine

BZA has an additional possibility for interaction with oxides because of its aromatic π-system. This property manifests itself on SiO_2 by the appearance of an IR band at 3631 cm^{-1}, indicative of the surface complex:

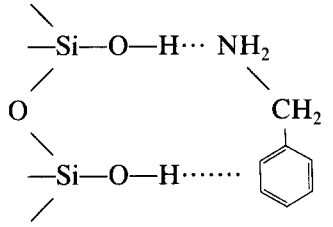

This two-point adsorption of aromatic compounds is found on SiO_2 (*26*) particularly, but has also been reported with other oxides (*27*). However, unambiguous evidence for the analogous surface complexes on Al_2O_3, Fe_2O_3, MgO, and CaO could not be detected in the present work. As with aliphatic *n*-amines, the desorption behavior of the BZA/oxide systems is mainly characterized by dehydrogenation of molecules coordinatively bonded to strong Lewis acid sites, giving benzonitrile in the case of BZA. A second reaction, indicated by NH_3 formation, is CN bond breakage, not observed with saturated aliphatic *n*-amines; this is probably caused (cf. AA) by the weaker CN bond in BZA (e.g., ethylamine D_{CN} = 352 kJ mol^{-1}; benzylamine D_{CN} = 301 kJ mol^{-1} (*28*)). On Fe_2O_3, simultaneously with the NH_3 desorption strong IR bands appear at 1589, 1526, and 1402 cm^{-1}, indicative of the oxidation of the intermediately formed benzyl species to adsorbed benzoate (*29*). All reactions occurring between 473 and 553 K (temperature range of TPD maximum FII; Fig. 5) can be summarized by the following scheme:

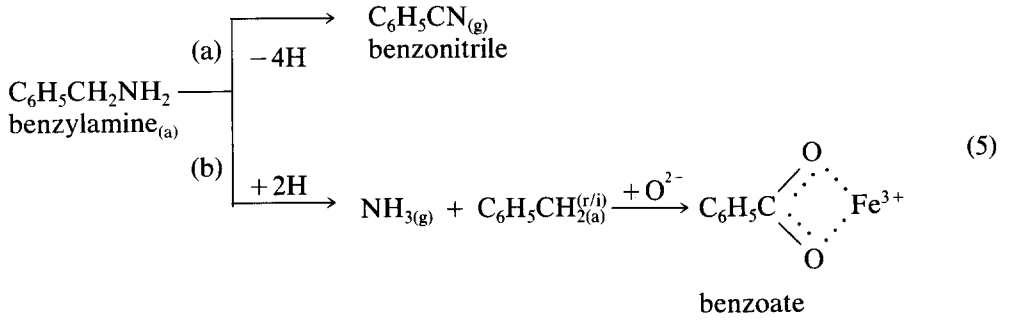

(5)

With a further temperature increase decarboxylation of adsorbed benzoate species takes place, which causes the desorption of benzene (TPD maximum FIII). Monitoring the partial pressure of CO_2 during the TPD run (shoulder at 643 K; further increase up to the strong maximum at 718 K) one can conclude that the products of this decarboxylation process (benzene, CO_2) desorb only in part, whereas the predominant portion of the formed benzene undergoes deep oxidation to CO_2 and H_2O on the Fe_2O_3 surface,

thus causing the strong TPD maximum FIV:

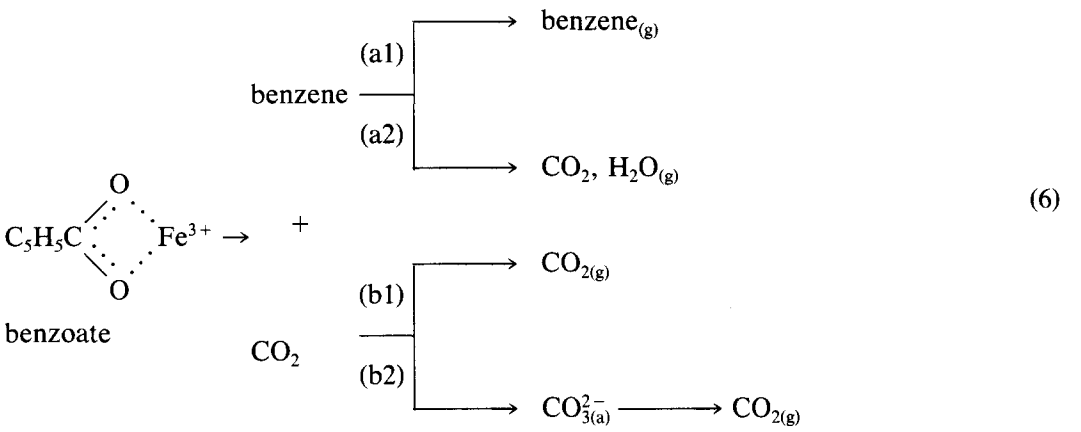

(6)

Considering the results of King and Strojney (*30*), reaction route (6-b2) is also possible, but not detectable in this case.

The fundamental work of Andersson (*31*) can serve as a corroboration of our notations of oxidation processes.

Using Al_2O_3, in principle the same reactions occur as with Fe_2O_3 (Eq. (5)). Contrary to Fe_2O_3, the desorption maximum of NH_3 appears at a temperature considerably lower than that of benzonitrile (Table 3). In the same temperature range dehydrogenation of BZA to adsorbed imine species begins, thus producing hydrogen necessary for the formation of NH_3. Another distinction consists in the fact that the benzyl species (formed according to Eq. (5b)) remain unchanged on the solid surface and are oxidized only in the temperature range of TPD maximum AII (Fig. 5). The latter process leads to the formation of adsorbed benzoate and carbonate species and causes desorption of benzene:

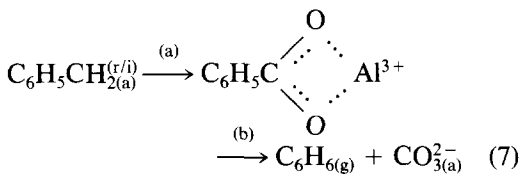

(7)

Oxidation of the benzyl species is indicated by IR bands at 1595, 1542, 1498, and 1432 cm^{-1}, which can be attributed unambiguously to adsorbed benzoate species (*32, 33*).

However, the band at 1432 cm^{-1} is more intense than would be expected according to the literature data. Together with the observed desorption of benzene, this phenomenon refers to a transformation of a part of the adsorbed benzoate species indicated by Eq. (7b), because the most intense i.r. band of the carbonate group is located near 1430 cm^{-1}. Such a reaction was also found, for example, during heating of Y_2O_3/benzoic acid adsorbates (*30*), and thermal decomposition of tetrabenzyl-metal-complexes yields benzene as a main product (*34*). Finally, analogous to Fe_2O_3 (Eq. (6)), thermal decomposition of the remaining benzoate species (and carbonate groups) causes TPD maximum AIII, comprising benzene and CO_2. The results concerning adsorption and reaction behavior of BZA on MgO, CaO, and SiO_2 can be interpreted in the same way. With MgO and CaO only reaction (5a) occurs (temperature range of TPD maximum CII; Fig. 5), whereas thermal decomposition of the secondary amine structure (formed by dissociative adsorption of BZA on strained siloxane bridges of SiO_2 (*1*)) additionally yields small amounts of other reaction products (methane, HCN).

CONCLUSION

In concluding this part, our work concerning the adsorption and reaction behavior of amines on oxides with different surface properties, some general conclusions about the studies as a whole can be made. The presented results provide knowledge in two main directions. On one hand, founded upon the investigation of a variety of amines some general effects of the molecular structure on their reactivities could be discovered, which allow predictions in the case of amines not investigated. Thus the favored reaction route consists in the formation of the corresponding nitriles (via adsorbed imine intermediates) by dehydrogenation only (primary *n*-amines (*35, 36*)) or dehydrogenation and dealkylation (secondary and tertiary amines (*1*)). If the structural conditions do not allow such chemical transformations, CN bond breakages dominate, leading to the evolution of alkenes and ammonia (amines with the NH_2 group located on secondary carbon atoms (*2*) and carbon atoms to which no hydrogen is attached (*3*), respectively). Using amines with weak CN bonds, both the above mentioned reactions occur simultaneously (allyl-, benzylamine). Many further chemical transformations can be observed, the nature of which depends on the structure, especially of the hydrocarbon residue, e.g., dehydrogenation of cyclic compounds (cyclohexylamine (*2*)), dimerization and cyclization (allylamine, ethylenediamine (*37*)), or decomposition (benzylamine) of relatively stable ionic or radical intermediates. These reactions only occur at elevated temperatures (with the exception of allylamine), result from the interaction of amine molecules with strong Lewis acid centers on the oxide surfaces, and are detectable not only during the TPD experiments but also in true catalytic flow systems.

On the other hand, these investigations clearly demonstrate the existence and activity of different surface centers of the oxides employed (discussed in Ref. (*1*)). Thus molecules that are hydrogen-bonded and coordinatively bonded to weak Lewis acid sites, respectively, do not undergo chemical transformations on the solid surfaces, whereas strong Lewis-acidic surface sites form such stable coordination bonds with amine molecules that the above mentioned reactions are initiated at elevated temperatures.

A special problem exists in the phenomenon that all amines are partly oxidized on Fe_2O_3. This process leads to the formation of adsorbed carboxylate groups, which are thermally stable up to ca. 700 K and resistent against the attack of, for example, water. Because of the dependence of the extent of oxidation on the molecular structure, these results could be of interest for the selection of amines as corrosion inhibitors.

REFERENCES

1. Sokoll, R., Hobert, H., and Schmuck, I., *J. Catal.* **121,** 153 (1990).
2. Sokoll, R., Hobert, H., and Schmuck, I., *J. Catal.* **125,** 276 (1990).
3. Sokoll, R., and Hobert, H., *J. Catal.* **125,** 285 (1990).
4. Rudakoff, G., Sokoll, R., Hobert, H., and Schmuck, I., *Z. Chem.* **27,** 150 (1987).
5. Fink, P., and Plotzki, I., "Wiss. Zeitschr. Friedrich-Schiller-Univ. Jena," Vol. 27, p. 69, 1978.
6. Oranskaja, O. M., Filimonov, V. N., and Schmuljakovski, Ya. E., *Kinet. Katal.* **11,** 1289 (1970).
7. Gordymova, T. A., and Davydov, A. A., *Kinet. Katal.* **20,** 733 (1979).
8. Davydov, A. A., *Mater. Chem. Phys.* **13,** 243 (1985).
9. Amenomiya, Y., and Cvetanovic, R. J., *J. Phys. Chem.* **67,** 2705 (1963).
10. Gordymova, T. A., and Davydov, A. A., *Dokl. Akad. Nauk SSSR* **245,** 635 (1979).
11. Dent, A. L., and Kokes, R. J., *J. Am. Chem. Soc.* **92,** 6709 (1970).
12. Klostermann, K., Diss. B, Jena, 1979.
13. Minachev, Ch.M., and Kondratjev, T. A., *Usp. Khim.* **52,** 1921 (1983).
14. Kitagawa, H., Sendoda, Y., and Ono, Y., *J. Catal.* **101,** 12 (1986).
15. Dadyburjor, D. B., Jewur, S. S., and Ruckenstein, E., *Catal. Rev.* **19,** 293 (1979).
16. Coluccia, S., Lavagnino, S., and Marchese, L., *J. Chem. Soc., Faraday Trans. 1* **83,** 477 (1987).
17. Garrone, E., and Stone, F. S., *in* "Proceedings,

8th International Congress on Catalysis, Berlin, 1984," Vol. 3, p. 441. Dechema, Frankfurt-am-Main, 1984.
18. Nelson, W. J., and Walmsley, D. G., "Vibrations at Surfaces," p. 471. Plenum, New York, 1982.
19. Sourisseau, C., Pasquier, P., and Hervieu, J., *Spectrochim. Acta A* **31,** 287 (1975).
20. Hattori, H., Tanaka, Y., and Tanabe, K., *J. Am. Chem. Soc.* **98,** 4652 (1976).
21. Miyahara, K., Murata, Y., Toyoshima, I., Tanaka, Y., and Yokoyama, T., *J. Catal.* **68,** 186 (1981).
22. Stone, F. S., Garrone, E., and Zecchina, A., *Mater. Chem. Phys.* **13,** 331 (1985).
23. Kawakami, H., and Yoshida, S., *J. Chem. Soc., Faraday Trans. 2* **80,** 921 (1984).
24. Garrone, E., Zecchina, A., and Stone, F. S., *J. Catal.* **62,** 396 (1980).
25. Ishiguro, J., *J. Pharmacol. Soc. Jpn.* **74,** 1100 (1954).
26. Pohle, W., *J. Chem. Soc., Faraday Trans. 1* **78,** 2101 (1982).
27. Zecchina, A., Coluccia, S., and Morterra, C., *Appl. Spectrosc. Rev.* **21,** 259 (1985).
28. Weart, R. C., "Handbook of Chemistry and Physics," 64th ed. C.R.C. Press, Boca Raton, FL, 1983.
29. Busca, G., Zerlia, T., Lorenzelli, V., and Girelli, A., *React. Kinet. Catal. Lett.* **27,** 429 (1985).
30. King, S. T., and Strojny, E. J., *J. Catal.* **76,** 274 (1982).
31. Andersson, S. L. T., *J. Catal.* **98,** 138 (1986).
32. Simonsen, M. G., Coleman, R. V., and Hansma, P. K., *J. Chem. Phys.* **61,** 3789 (1974).
33. Niwa, M., Inagaki, S., and Murakami, Y., *J. Phys. Chem.* **89,** 2550 (1985).
34. Köhler, E., Brüser, W., and Thiele, K.-H., *J. Organomet. Chem.* **76,** 235 (1974).
35. Marx, U., Sokoll, R., and Hobert, H., *J. Chem. Soc., Faraday Trans. 1* **82,** 2505 (1986).
36. Sokoll, R., Hobert, H., and Schmuck, I., *J. Chem. Soc., Faraday Trans. 1* **82,** 3391 (1986).
37. Sokoll, R., unpublished results.